Joint Estimation of Linear and Non-linear Signal-to-Noise Ratio based on Neural Networks

F.J. Vaquero Caballero[(1)], David Ives[(1)], Qunbi Zhuge[(2)], Maurice O'Sullivan[(2)], Seb J. Savory[(1)]

[(1)] *University of Cambridge, 9 JJ Thomson Avenue, Cambridge, CB3 0FA, U.K.*
[(2)] *Ciena Corporation, Ottawa, ON, Canada*
Email: fjv24@cam.ac.uk

Abstract: A novel technique estimating ASE and non-linear SNR is presented. Our method is evaluated by simulations obtaining a std error of 0.23 dB for both ASE and non-linear SNR.

OCIS codes: (060.4510) Optical communications; (120.3940) Metrology.

1. Introduction

Traffic demand is growing, increasing the pressure on operators to maximize the capacity over the deployed networks. Flexible Optical Networking and Impairment Aware Networking will heavily rely on signal quality information for routing decisions, which will be required to be estimated *a posteriori* due to the heterogeneity and complexity of networks. Optical Performance Monitoring (OPM) is the research field aiming to characterize the impairments suffered over transmission from the received signal.

Optical communication links comprise of several spans of optical fibre followed by noisy Erbium doped fibre amplifiers (EDFA), compensating for signal loss. During transmission, the received signal is affected by different impairments: inter-symbol interference (ISI) from the induced chromatic dispersion (CD), state-of-polarization rotation (SOPR), amplified spontaneous emission noise (ASE) and non-linear interference noise (NLI). The origins of ASE and NLI are fundamentally different: while ASE is produced by spontaneous emission by EDFAs and is independent of the signal, NLI is caused by the interaction of electromagnetic fields in silica glass and is proportional to the cube of the signal power (p) multiplied by a non-linear efficiency factor η_{NL} [1].

CD and SOPR are compensated at the receiver by the equalizer in the Digital Signal Processing (DSP) block incurring insignificant penalties [2]; ASE cannot be similarly compensated and in-band NLI can be compensated by perturbation-based precompensation [3] or digital back-propagation [4], with both algorithms expensive in terms of computations. Thus, ASE and NLI limit the symbol rate, reach, and modulation format of the signal. The signal-to-noise ratio (SNR) dictates the overall maximum achievable capacity of a given link and is the *de facto* figure of merit of any communication system:

$$SNR^{-1} = \frac{ASE}{p} + \frac{\eta_{NL} p^3}{p} = SNR_{ASE}^{-1} + SNR_{NLI}^{-1} \tag{1}$$

Current research focuses on different definitions of the amplitude noise covariance to estimate the NLI based on linear regressions [5] or Neural Networks (NN) [6]. Others jointly estimate both ASE and NLI, by performing a fitting between the transmitted power and the received SNR requiring varying the power of the transmitted signal [1] and so doing compromising the quality of the transmitted signal.

This paper presents a novel technique capable of simultaneously estimating NLI and ASE, with similar complexity to previous approaches. The proposed technique is transparent to transmitter and receiver: without relying on power variations or requiring special training sequences. We evaluated our method with extensive computer simulations and we observed it is capable of estimating both the ASE and NLI with a standard deviation (std) error of 0.23 dB for both SNR_{NLI} and SNR_{ASE}.

2. The proposed technique

A typical 16-QAM noisy signal constellation is illustrated in Figure 1 with the 3 constellation rings attributed to different power levels. The noise for each constellation symbol can be decomposed in its tangential, $\mathbf{t}$, and normal, $\mathbf{n}$, components. Its noise components are approximately constant for each symbol within a ring but varies from ring to ring. ASE produces symmetric Gaussian noise with tangential and angular components independent of the symbol. On the other hand, NLI is power dependent and, for advance modulation formats, a large contribution can be characterized as non-linear phase noise [7], manifesting as correlated noise and producing non-circular variations along the different $\mathbf{t}$ and $\mathbf{n}$ components. Averages of the $\mathbf{t}$ and the $\mathbf{n}$ components are calculated for each ring, resulting in $\mathbf{T}_r^h$ and $\mathbf{N}_r^h$;

$\forall\, h = \{1,2,3\}$. Figure 2 shows the behaviour of the proposed metrics in simulations and experiments for 800km of True-Wave Classic fibre (TWC). By incrementing the transmitted power, NLI is also increased and the contributions of $\mathbf{T}_r^2$ and $\mathbf{T}_r^3$ have a more pronounced growth than the rest of contributions. The normal components also show a different evolution by varying the transmitted power: $\mathbf{N}_r^3$ component experiments a steeper growth than $\mathbf{N}_r^1$ and $\mathbf{N}_r^2$. The described evolution of the noise components takes place even after carrier-phase estimation (CPE), indispensable for processing the included experimental data.

Based on [7], we do not expect the resultant NLI to be circularly symmetric Gaussian for 16-QAM with 16-QAM interfering channels, in contrast to QPSK signals with QPSK interfering channels, where NLI is expected to be almost circularly symmetric Gaussian. In this paper we also show that in the scenarios considered for 16-QAM, NLI is far from having a circular symmetric Gaussian distribution.

The other metrics used in this paper are the amplitude noise covariance (ANC) and its accumulative logarithmic ANC (ALANC). The amplitude noise of an x-polarization symbol-k ($\Delta s_{k,x}$) is the difference between expected and received symbols for the x-polarization: $|s_{k,x}|$-$|\hat{s}_{k,x}|$, the amplitude noise correlation of y-polarization ($\Delta s_{k,y}$) is defined accordingly. The introduced metrics are calculated as:

$$ANC_{ij}(m) = cov(\Delta s_{k,i}, \Delta s_{k+m,j}), \qquad ALANC_{ij} = 10\log_{10}(1/\sum_{i=1}^{6}|ANC_{ij}(i)|), \qquad i,j \in \{x,y\} \tag{2}$$

The presented metrics: $\mathbf{T}_r^h$, $\mathbf{N}_r^h$, $ALANC_{xx}$ and $ALANC_{xy}$, in combination with ACD and number of WDM channels (nWDM), are used as input of a NN, consisting of 1 hidden layer and 7 neurons (Figure 3). The NN network uses an hyperbolic tangent sigmoid as non-linear function, $g(x)$, and is trained by the 70/15/15 rule for the train/dev/test with early stopping over the dev.

Figure 4 plots the ALANC metric, $\mathbf{T}_r^h$, and $\mathbf{N}_r^h$ against SNR_{NLI} illustrating the need of a NN as an estimator of their non-linear relationship. Table 1 summarizes the 2160 cases considered for the training and validation of our algorithm. The 35 Gbaud, DP-16QAM with a 0.14 roll-off factor was transmitted over different WDM configurations, fibres types, and lengths. The 50 GHz spaced WDM system was simulated as noise-free, while ASE was loaded into the receiver according to several ASE-to-NLI power ratios (ANR), comprising the optimum operation point, $ANR = 2$, and another 4 cases: 0.5, 1, 4 and 8.

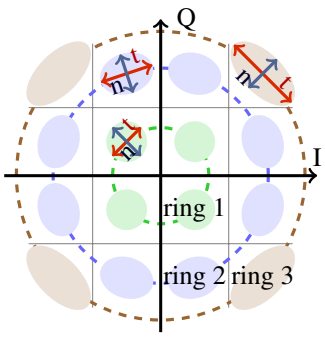

Fig. 1: 16-QAM signal and **t** and **n** components.

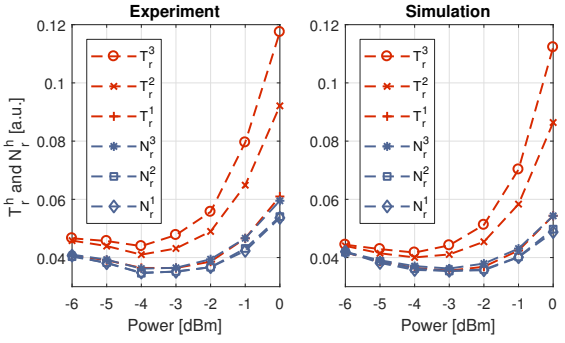

Fig. 2: $\mathbf{T}_r^h$ and $\mathbf{N}_r^{1:3}$ for 11xDWDM over 800km of TWC.

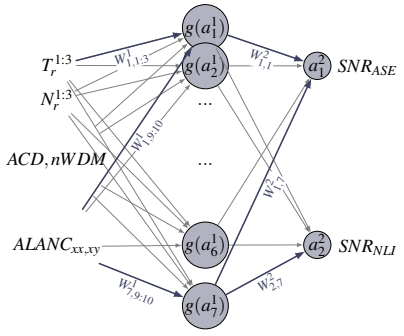

Fig. 3: Structure of the implemented NN (biases are omitted).

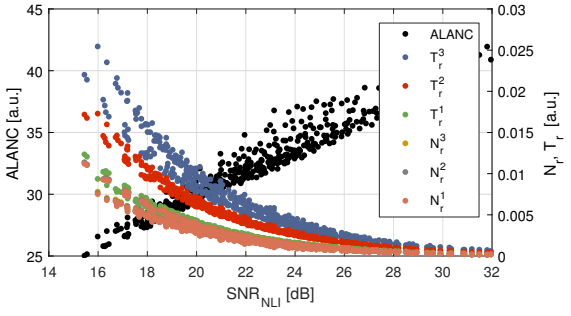

Fig. 4: Evolution of ALANC and T_r^h and N_r^h for all the simulation data.

Fibre types	NDSF	TWC	ELEAF	NDSF & TWC	NDSF & ELEAF	ELEAF & TWC
Channel launch power [dBm]	0.5	-2.5	-1	-1	-0.5	-2
Distance [km]	320, 400, 480, 560, 640, 720, 800, 880, 960, 1040, 1120, 1200					
WDM channel	1, 3, 5, 7, 11, 21					
ASE-to-NLI ratio	0.5, 1, 2, 4, 8					

Table 1: Scenarios considered for the proposed technique

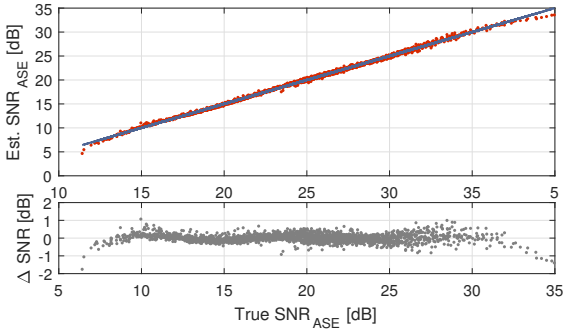

Fig. 5: True vs estimated SNR_{ASE}.

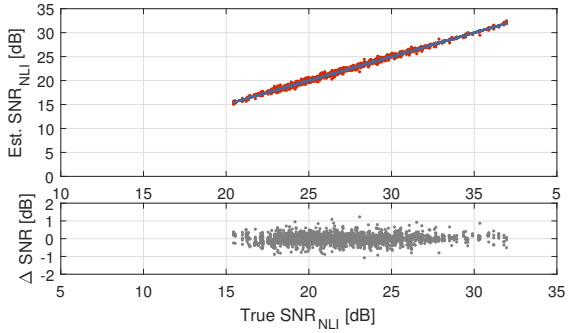

Fig. 6: True vs estimated SNR_{NLI}.

3. Results

Figure 5 and 6 shows the true vs estimated SNR_{ASE} and SNR_{NLI}, respectively. Good agreement between expected and estimated values is observed corresponding to a std error of 0.23 dB. Several iterations are performed over the NN with different initializations of the weights. The possibility of over-fitting was minimized by evaluating the error of the three data sets and ensuring that the solution does not suffer from bias or variance errors. Although solutions in which one of the estimates can have a smaller estimation error at expense of the other are possible, we aimed for solutions with approximately same performance for both estimates. We evaluated the performance under CPE, by loading phase noise equivalent of 200 kHz of linewidth over the simulated data and recovering the resultant signal with a modified Viterbi&Viterbi, the NN was then trained with the metrics influenced by residual phase noise and was capable of estimating SNR_{ASE} and SNR_{NLI} with a std of 0.31 dB. The CPE analysis was limited to an SNR $>$10 dB, suppressing 106 signals, corresponding to the cases where the pre-FEC bit error rate exceeded 6%. Finally, we tested the performance of the NN trained without $\mathbf{T}_r^h$, or $\mathbf{N}_r^h$, obtaining a std error 0.39 and 0.25 dB, respectively.

4. Conclusion and future work

We developed and evaluated a novel technique for jointly estimating SNR_{ASE} and SNR_{NLI} with std error of 0.23 dB over a wide range of fibres, ASE-to-NLI ratios, WDM channels, and distances. The proposed metric is simple, requiring the extraction of basic features of the post-DSP signal and a small Neural Network suitable for its implementation in receivers. Its performance was also validated under the influence of CPE and phase noise. Future work will include the experimental evaluation of the proposed technique.

Acknowledgements: FJVC, DI, and SJS thank Ciena and UK EPSRC (through the project INSIGHT EP/L026155/2) for funding and support.

References

1. D.J. Ives, et al., "Single Channel Probe Utilizing the EGN Model to Estimate Link Parameters for Network Abstraction," Proc. ECOC 17, P2.SC6.13 (2017)
2. Seb J. Savory, "Digital filters for coherent optical receivers," Opt. Express 16, 804-817 (2008)
3. Y. Gao, et al., "Reducing the complexity of perturbation based nonlinearity pre-compensation using symmetric EDC and pulse shaping," Opt. Express 22, 1209-1219 (2014)
4. C.B. Czegledi, et al., "Digital backpropagation accounting for polarization-mode dispersion," Opt. Express 25, 1903-1915 (2017)
5. Z. Dong, et al.,"OSNR monitoring for QPSK and 16-QAM systems in presence of fiber nonlinearities for digital coherent receivers," Opt. Express 20, 19520-19534 (2012)
6. A.S. Kashi, et al., "Fiber Nonlinear Noise-to-Signal Ratio Monitoring Using Artificial Neural Networks," Proc. ECOC 17, M.2.F.2 (2017)
7. R. Dar, et al., "Properties of nonlinear noise in long, dispersion-uncompensated fiber links," Opt. Express 21, 25685-25699 (2013)